

# Preparation of (In,Mn)As/(Ga,Al)Sb magnetic semiconductor heterostructures and their ferromagnetic characteristics

H. Munekata, A. Zaslavsky, P. Fumagalli,<sup>a)</sup> and R. J. Gambino  
IBM Research Division, T.J. Watson Research Center, P.O. Box 218, Yorktown Heights,  
New York 10598

(Received 21 June 1993; accepted for publication 23 September 1993)

A series of III-V-based magnetic semiconductor heterostructures, *p*-type (In,Mn)As/(Ga,Al)Sb, has been grown by molecular beam epitaxy. Studies on magnetotransport and magneto-optical properties show that perpendicular ferromagnetic order occurs in the heterostructures with thin (In,Mn)As layers. The origin is discussed in terms of both carrier- and strain-induced effects.

(In,Mn)As is a new III-V-based diluted magnetic semiconductor with interesting properties associated with carrier-induced magnetism. It has been shown that the spin exchange between holes and Mn ions in *p*-type  $\text{In}_{1-x}\text{Mn}_x\text{As}$  ( $x=0.01-0.02$ ) films causes an anomalous Hall effect over a wide temperature range (1.6–200 K). Carrier-induced partial ferromagnetic order is observed below 10 K.<sup>1</sup> In this letter, we report on the striking ferromagnetic order, accompanied by a strong perpendicular anisotropy, in *p*-(In,Mn)As/(Ga,Al)Sb heterostructures with thin (5–30 nm) *p*-(In,Mn)As layers. These heterostructures were grown by molecular beam epitaxy (MBE). The appearance of perpendicular ferromagnetic order as a function of (In,Mn)As thickness is demonstrated by low-field Hall measurements, while the hole concentration and mobility are extracted from high-field magnetotransport data. Magneto-optical properties are examined by polar Kerr rotation experiments, through which we show that the rotation is relatively large (0.1–0.2°) and has complex wavelength and thickness dependencies. On the basis of the dependencies of ferromagnetic behavior on (In,Mn)As thickness and GaSb-based buffer alloy composition, we propose that the observed perpendicular ferromagnetic order results from the combination of carrier-induced and magnetoelastic effects, in biaxially strained (In,Mn)As layers.

We grew (In,Mn)As/(Ga,Al)(Sb,As)/GaSb/GaAs structures on GaAs(100) substrates, with the thickness of each constituent layer ranging from 3 nm to 1 μm, 0.13–0.3 μm, 0.3–1.2 μm, and 0.3 μm, from the top (In,Mn)As to the bottom GaAs buffer, respectively. Here, the (Ga,Al)(Sb,As) indicates either binary GaSb or AlSb compounds, or ternary (Ga,Al)Sb or Al(Sb,As) alloys. Mn fraction  $x$  in the  $\text{In}_{1-x}\text{Mn}_x\text{As}$  layer ranged between 0.04 and 0.15. The substrate temperature  $T_s$  for the growth of nonmagnetic III-V layers was  $T_s=480-580^\circ\text{C}$ , whereas  $T_s=170-200^\circ\text{C}$  for the (In,Mn)As layers. The low- $T_s$  growth yields a homogeneous (In,Mn)As film in the zincblende structure without the macroscopic ferromagnetic MnAs second phase, as confirmed recently by transmission electron diffraction studies for thick ( $>2\ \mu\text{m}$ )

bulk-type films.<sup>2</sup> X-ray absorption fine-structure (XAFS) measurements show that Mn atoms form small ( $r\sim 3\ \text{\AA}$ ) MnAs<sub>6</sub> centers.<sup>3</sup> MBE growth was interrupted for 10 min after (Ga,Al)(Sb,As) deposition to allow  $T_s$  reduction/stabilization, under which no beam flux impinged on the as-grown (1×3) reconstructed (Ga,Al)(Sb,As) surface. The (In,Mn)As growth usually proceeded with a reasonably smooth surface with the (1×1) structure, although we found a tendency for three-dimensional island growth under either high As<sub>4</sub> or high Mn (for  $x>0.1$ ) beam pressure. Typical As<sub>4</sub>/(In+Mn) ratio was  $\sim 2$  with an (In,Mn)As growth rate of 2.2 Å/s.

Low-field Hall effect measurements at room temperature indicate that all the films grown on GaSb-based layers are *p* type. This is in contrast to previous *n*-type samples grown at the same low  $T_s$  on thin (20–50 nm) InAs buffer layers.<sup>4</sup> On the other hand, it has been shown that the growth on the InAs/GaAs at relatively high temperatures,  $T_s=275-300^\circ\text{C}$ , suppressed the formation of *n*-type defects, resulting in activation of holes from Mn ions.<sup>5</sup> The problem of this method, however, was the development of MnAs second phase at Mn composition  $x$  as low as  $x\sim 0.03$ . The role of relatively thick GaSb-based buffer layers (0.3–1.2 μm) is presumably to improve the electronic quality of the (In,Mn)As epilayers by reducing significantly the generation of *n*-type crystal defects during the growth of (In,Mn)As even at low  $T_s$ . We have also observed the same buffer-layer dependence on the electrical conduction for *n*/*p*-InAs:Be layers grown under the low  $T_s$ . The absence of the macroscopic ferromagnetic MnAs second phase was confirmed by magnetization measurements of 1-μm-thick films.

Figure 1 shows low-field Hall resistance ( $R_{\text{Hall}}$ ) curves at 4.2 K for (In,Mn)As/AlSb samples with different (In,Mn)As thicknesses  $d_{\text{MS}}$ , and Mn fraction  $x\sim 0.07$ . The  $R_{\text{Hall}}$  curve with  $d_{\text{MS}}=1\ \mu\text{m}$  exhibits *p*-type behavior with a slight nonlinear feature, showing weak ferromagnetic characteristics. A rounded magnetization ( $M$ - $H$ ) curve, reflecting ferromagnetic behavior, is also observed in the high-field magnetization measurement of this sample. The weak remanent magnetization previously observed in the *p*-type  $x=0.01-0.02$  samples,<sup>1</sup> is absent in the  $x=0.07$  sample. The reduction of the (In,Mn)As layer thickness causes a significant change in the transport characteristics: Strong nonlinearity appears for  $d_{\text{MS}}=100\ \text{nm}$  and, with

<sup>a)</sup>Present address: 2. Physikalisches Institut, RWTH Aachen, Templergraben 55, 5100 Aachen, Germany.

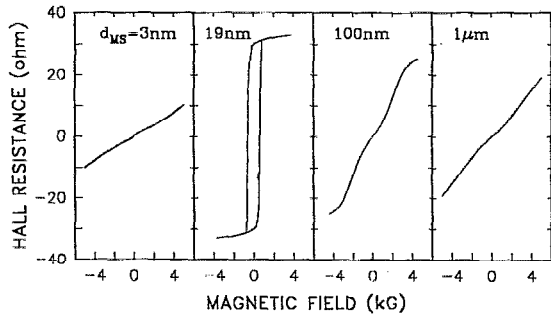


FIG. 1. Development of square loop hysteresis in the Hall resistance as a function of (In,Mn)As layer thickness  $d_{MS}$  in  $p$ -(In,Mn)As/AlSb heterostructures. Mn fraction is  $x \sim 0.07$ , and  $T = 4.2$  K.

$d_{MS}$  further reduced, a square hysteresis loop develops below  $d_{MS} \sim 30$  nm (see Fig. 1). In this thickness regime, the  $R_{Hall}$  is apparently governed by the anomalous Hall term, and thus by the extent of magnetization. The square loop indicates a well-aligned ferromagnetic order with a strong magnetic anisotropy perpendicular to the (100) film plane. This character is preserved with  $d_{MS}$  down to 5 nm, below which it disappears. A slight nonlinearity, however, remains in the Hall resistance curve at  $d_{MS} = 3$  nm (Fig. 1). The magnitude and width of the square loop become smaller with increasing temperature. From the vanishing point of remanent magnetization, a Curie temperature  $T_C$  is determined to be about 30–35 K for the sample with  $d_{MS} \sim 10$  nm, below and above which  $T_C$  tends to decrease.

For samples with perpendicular ferromagnetic order, it was possible to extract carrier concentrations from the Hall data taken below 10 K and above 150 K under high fields (6–10 T). Under such conditions, changes in Hall resistance arise from the ordinary Hall effect because of fairly quick magnetization saturation when  $T < 10$  K, and very small magnetic susceptibility when  $T > 150$  K, respectively. For the temperature range in between, the susceptibility is fairly large and the Hall resistance curve is strongly affected by the anomalous Hall term. Three Hall resistance curves in each temperature range are shown in Fig. 2 for 9 nm-(In,Mn)As/GaSb, together with magnetoresistance curves (inset). Mn composition of the (In, Mn)As layer is  $x \sim 0.1$ . Carrier density  $p$  and mobility  $\mu_p$  of this sample are summarized in Table I, from which we find that  $p$  at high temperatures ( $> 180$  K) tends to saturate at a constant value ( $p = 9 \times 10^{13} \text{ cm}^{-2}$ ), whereas a part of carriers freezes out at low temperatures ( $p = 5.2 \times 10^{13} \text{ cm}^{-2}$  at 4.2 K). Carrier densities of other ferromagnetic heterostructures ranged from mid  $10^{13}$  to low  $10^{14} \text{ cm}^{-2}$ , e.g.,  $p = 1.4 \times 10^{14} \text{ cm}^{-2}$  at 4 K for 19 nm-(In, Mn)As/AlSb heterostructure in Fig. 1. The  $\mu_p$  values of ferromagnetic heterostructures are  $\mu_p = 60$ – $120 \text{ cm}^2/\text{V s}$  at 4 K, relatively high compared to that of  $p$ -type bulk samples (e.g.,  $\mu_p \sim 2.4 \text{ cm}^2/\text{V s}$  at 10 K, Ref. 1). This may be explained in terms of the relation between spin alignment and carrier localization. In the heterostructure, Mn spins are fully aligned so that magnetic homogeneity is quite high compared to that in the partially aligned spins in bulk  $p$ -type

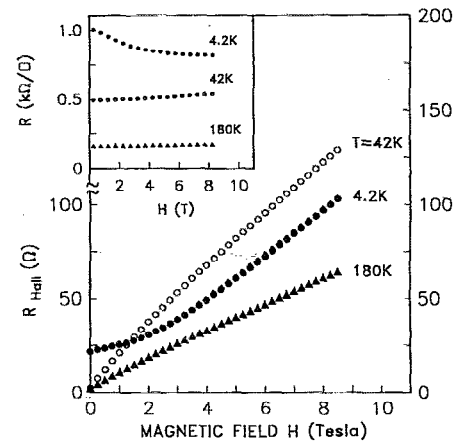


FIG. 2. Hall resistance curves of the 9 nm-(In,Mn)As/GaSb heterostructure at different temperatures. Mn fraction is  $x \sim 0.10$ . Inset figure shows magnetoresistance curves.

samples.<sup>1</sup> Because of this fact, holes in the heterostructures will be less affected by a magnetically driven localization effect.

In polar Kerr rotation measurements, a square hysteresis is observed throughout the entire energy region (0.7–3.0 eV), consistent with transport data in Fig. 1. The spectra exhibit relatively large magneto-optical (MO) effect with rather complicated wavelength dependence, as shown in Fig. 3. We find that in the energy region below 1.5 eV both peak position and amplitude depend sensitively on (In,Mn)As and AlSb layer thicknesses. Since both layers are virtually transparent in this energy region, we expect a large contribution to the MO effect from optical interference involving (In,Mn)As and dielectric layers (AlSb, GaSb). In contrast, for the structures above 1.5 eV, only peak amplitudes are affected by changes in layer thicknesses. In particular, the sharp peak at  $\sim 1.75$  eV becomes much weaker as (In,Mn)As layer thickness is increased from 9–10 nm (Fig. 3). The s-shaped structure at  $\sim 2.5$  eV appears to be less affected. We believe<sup>6</sup> that the MO effect of a thin (In,Mn)As layer is enhanced at  $\sim 1.75$  eV by the optical coupling with the direct band gap of AlSb ( $E_g = 2.2$  eV). In other words, a large change in optical functions of AlSb near its band gap strongly influences the overall Kerr rotation  $\Theta_K$ , as suggested in metal multilayers in terms of plasma-edge enhancement.<sup>7</sup> The maximum  $\Theta_K$  value ob-

TABLE I. Zero-field resistance  $R_0$ , carrier density  $p$ , and mobility  $\mu_p$  of 9 nm-(In,Mn)As/GaSb ( $x \sim 0.1$ ) extracted from high field (6–10 T) data at different temperatures.

$T$ (K)	$R_0$ ( $\Omega/\square$ )	$p$ ( $10^{13} \text{ cm}^{-2}$ )	$\mu_p$ ( $\text{cm}^2/\text{V s}$ )
1.6	1255	4.6	108
4.2	1000	5.2	121
135 <sup>a</sup>	193	6.9	466
152	172	7.4	489
180	157	9.1	435
$RT$ <sup>b</sup>	261	9.3	257

<sup>a</sup>Hall resistance shows slight nonlinear behavior.

<sup>b</sup>Measurement done for  $0 < H < 1$  T.

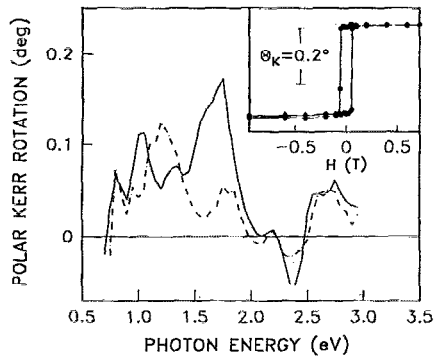


FIG. 3. Remanent polar Kerr rotation spectra at 5.5 K for two heterostructures with different structural parameters: 9 nm-(In,Mn)As/136 nm-AlSb with  $x=0.1$  (solid line), and 19 nm-(In,Mn)As/195 nm-AlSb with  $x=0.07$  (dashed line). Curie temperatures are  $T_C \sim 35$  and 17 K, respectively. Inset figure shows a square hysteresis loop at  $h\nu=1.75$  eV.

tained so far is  $\Theta_K=0.18^\circ$  at 1.75 eV from the 9 nm-(In,Mn)As/AlSb structure. With this value, specific Faraday rotation is estimated to be about  $10^5$  deg/cm at full saturation, assuming double Faraday rotation<sup>8</sup> of reflected light at the (In,Mn)As/AlSb interface.

We now discuss the origin of perpendicular ferromagnetic order. While perpendicular ferromagnetic order exists in thin (In,Mn)As/Ga<sub>1-y</sub>Al<sub>y</sub>Sb for the entire range of  $0 < y < 1$ , it is significantly weaker in (In,Mn)As/AlSb<sub>1-z</sub>As<sub>z</sub> structures and vanishes with As fraction of  $z \sim 0.15$ . This As value gives a nearly lattice-matched condition between the two constituent layers. Based on this alloy composition dependence, together with thickness-dependent ferromagnetic behavior (Fig. 1), we attribute the observed anisotropy to a strain-induced crystal anisotropy caused by the lattice mismatch (0.6%–1.3%) between (In,Mn)As and (Ga,Al)Sb layers. A thin (In,Mn)As layer on (Ga,Al)Sb is under biaxially tensile strain, resulting in the magnetoelastic effect along the  $\langle 001 \rangle$  direction to appear in the layer. The sign of magnetoelastic constant  $\lambda$  is then positive, since (In,Mn)As lattices are compressed along the  $\langle 001 \rangle$  direction. Increasing  $d_{MS}$  beyond the critical thickness (about 55 nm for (In,Mn)As/AlSb<sup>9</sup>) leads to strain relief, and the magnetoelastic effect disappears. What is left in thick (In,Mn)As layers is a local magnetic coupling  $JS \cdot s$  between Mn( $S$ ) and hole ( $s$ ) spins.<sup>1</sup>

The disappearance of ferromagnetic order for

(In,Mn)As films thinner than 5 nm (Fig. 1) suggests the presence of another mechanism in the very thin layers. One intriguing possibility is hole transfer between (In,Mn)As and (Ga,Al)Sb. The Fermi level at the (In,Mn)As surface is assumed to be pinned above the conduction-band edge, as in InAs.<sup>10</sup> In addition, the valence-band edge of (Ga,Al)Sb is expected to lie above that of (In,Mn)As, similar to the band alignment in InAs/(Ga,Al)Sb heterostructures.<sup>11</sup> The consequence of these two conditions is that the hole wave function spreads over both (In,Mn)As and (Ga,Al)Sb layers.<sup>12</sup> When the (In,Mn)As layer thickness becomes comparable to the surface depletion width (2–3 nm, Ref. 13), the number of holes decreases, and the hole wave function is displaced from the (In,Mn)As toward the AlSb layer. Consequently, the disappearance of a square loop in the  $R_{Hall}$  of the 3 nm-(In,Mn)As/AlSb (see Fig. 1) can be explained by the lack of sufficient number of holes in the (In,Mn)As layer, rather than by the change in the strain-induced magnetic anisotropy.

In summary, we demonstrated the occurrence of perpendicular ferromagnetic order in MBE-grown  $p$ -(In,Mn)As/(Ga,Al)Sb heterostructures. These results indicate that the modification of both magnetic and semiconductor properties is possible in the III-V-based magnetic semiconductor heterostructure system. This work is supported in part by the Army Research Office and Office of Naval Research (Grant No. 0001492-C-0017).

<sup>1</sup>H. Ohno, H. Munekata, T. Penney, S. von Molnár, and L. L. Chang, Phys. Rev. Lett. **68**, 2664 (1992).

<sup>2</sup>S. Guha and H. Munekata, J. Appl. Phys. **74**, 2974 (1993).

<sup>3</sup>A. Krol, Y. L. Soo, S. Huang, Z. H. Ming, Y. H. Kao, H. Munekata, and L. L. Chang, Phys. Rev. B **47**, 7187 (1993).

<sup>4</sup>H. Munekata, H. Ohno, R. R. Ruf, R. J. Gambino, and L. L. Chang, J. Cryst. Growth **111**, 1011 (1991).

<sup>5</sup>H. Munekata, T. Penney, and L. L. Chang, Surf. Sci. **267**, 342 (1992), and references therein.

<sup>6</sup>P. Fumagalli, H. Munekata, and R. J. Gambino, IEEE Trans. Magn. (to be published).

<sup>7</sup>T. Katayama, Y. Suzuki, H. Awano, Y. Nishihara, and N. Koshizuka, Phys. Rev. Lett. **60**, 1426 (1988).

<sup>8</sup>See, e.g., E. Hecht and A. Zajac, *Optics* (Addison-Wesley, Reading, 1987), p. 316.

<sup>9</sup>R. People and J. C. Bean, Appl. Phys. Lett. **47**, 322 (1985); B. W. Dodson and J. Y. Tsao, Appl. Phys. Lett. **51**, 1325 (1987).

<sup>10</sup>S. Kawaji and H. C. Gatos, Surf. Sci. **7**, 215 (1967).

<sup>11</sup>L. F. Luo, R. Beresford, and W. I. Wang, Appl. Phys. Lett. **55**, 2023 (1989).

<sup>12</sup>F. Stern and S. E. Laux (private communications).

<sup>13</sup>The surface depletion region is estimated to be 2–3 nm, assuming a barrier height of 0.4 eV with ionized acceptors of  $5\text{--}10 \times 10^{19} \text{ cm}^{-3}$ .